THE JOURNAL OF PHYSICAL CHEMISTRY C

Article

pubs.acs.org/JPCC

Nanopatterning on H-Terminated Si(111) Explained as Dynamic Equilibrium of the Chemical Reaction with Methanol

Peter Thissen,*[,†] Ehud Fuchs,[‡] Katy Roodenko,[§] Tatiana Peixoto,[§] Ben Batchelor,[§] Dennis Smith,[§] Wolf Gero Schmidt,[∥] and Yves Chabal[§]

[†]Karlsruhe Institute of Technology (KIT), Institut für Funktionelle Grenzflächen (IFG), Hermann-von-Helmholtz-Platz 1, 76344 Eggenstein-Leopoldshafen, Germany

[‡]Zyvex Laboratories LLC, Richardson, Texas 75081, United States

[§]Department of Materials Science and Engineering, University of Texas at Dallas, 800 West Campbell Road, Richardson, Texas 75080, United States

[∥]Lehrstuhl für Theoretische Physik, Universität Paderborn, 33098 Paderborn, Germany

ABSTRACT: Here the microscopic mechanism that leads to the surprising formation of a nanopattern upon methanol reacting with a H-terminated Si(111) surface [Michalak et al., *Nat. Mater.* **2010**, *9*, 266−271] is reinvestigated from both theory and experiment. First-principles calculations determine the fully OCH_3-terminated Si(111) surface as the thermodynamic ground state in the presence of methanol, seemingly in contrast to the experimentally found nanopattern. At 65 °C the presence of H_2 initiates desorption of the methoxy groups and thereby leads to a dynamic equilibrium of the reaction of methanol with the H-terminated Si(111) surface, which is a 1/3 OCH_3-terminated and 2/3 H-terminated Si(111) surface, with all OCH_3 groups standing as NNNs, corresponding to the nanopattern observed earlier. Investigating fluorine group termination of Si(111) as a test system the present study demonstrates that the combination of theoretical and experimental techniques used here is in fact sufficiently sensitive to resolve complex molecular systems even with lateral resolution.

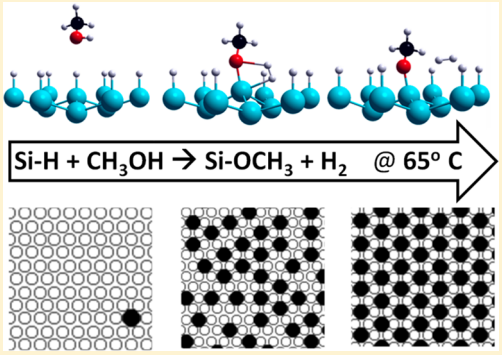

INTRODUCTION

The chemistry of surfaces and interfaces is an important factor in the fabrication of novel functional materials.[1−3] Patterning is one of the most challenging steps in the fabrication of micro- and nanoscale devices. The creation of surface patterns is particularly necessary for the synthesis of chemical/biological sensors and molecular electronic devices. Patterned surfaces with spatially ordered chemical functionalities comprise common technologies in fields such as optoelectronics and field-effect devices. The corresponding technologies are not without adversity and face challenges related to the pattern resolution, efficiency, and cost. Therefore, the development of both high-resolution and throughput fabrication methods that minimize the number of processing steps is highly desirable and important.

In general, the exchange approach is a powerful tool in interface engineering, displaying a great potential for tailoring of device characteristics. Lenz et al.[4] compared the kinetics of monolayer self-assembly long-chained carboxylic acids and phosphonic acids on thin aluminum oxide surfaces and investigated their dielectric properties in capacitors and low-voltage organic thin-film transistors. Phosphonic acid anchor groups tend to substitute carboxylic acid molecules on aluminum oxide surfaces and thus allow for the formation of mixed or fully exchanged monolayers. In a cross experiment under comparable conditions it was found that the exchange reaction only occurs from carboxylic acid to phosphonic acid and not vice versa.

Recently, Michalak et al. reported that immersion of atomically smooth Si(111):H surfaces in neat anhydrous CH_3OH at 65 °C for 12 h yields high-quality surfaces with <30% of monolayer Si−OCH_3 moieties, each being surrounded by six nearest-neighbor Si−H sites.[5−7] The perfection of the surface imparts its remarkable properties, highlighting the importance of oxide-free surfaces, and makes it possible to model reactivity, stability, and dielectric properties (interfacial charge transfer) using first-principles calculations.[8−11] However, the mechanism that leads to this very regular nanopattern remains an open question. In particular the theoretical prediction that a full 100% surface coverage of Si−OCH_3 sites is the most energetically favorable coverage for the Si(111) surface[12] seemingly contradicts the experimental observation of a maximum surface coverage density of ∼1/3 of a monolayer.[5]

Received: April 21, 2015
Revised: June 23, 2015
Published: June 23, 2015

DOI: 10.1021/acs.jpcc.5b03816
J. Phys. Chem. C 2015, 119, 16947−16953

Here, we reinvestigate this system and determine the optimum conditions for achieving a uniform surface density coverage of methoxy groups on the Si surface. At 65 °C the sheer presence of dihydrogen initiates the desorption of methoxy groups and thus leads to a dynamic equilibrium of the methoxylation of the Si(111) surface that is suitable to explain the experimental findings. At temperatures higher than 100 °C the decomposition of methanol in reflux conditions is found to play an important role, increasing the presence of chemical species initiating the oxidation of the surface.

METHODS

Sample Preparation. The following analytical grade chemicals were purchased and used as received: aqueous hydrogen peroxide, 30% by weight (H_2O_2, Fisher Scientific, 30%), sulfuric acid (H_2SO_4, Fisher Scientific, 18M), CMOS grade hydrofluoric acid (HF, J.T. Barer, 49%), CMOS grade ammonium fluoride (NH_4F, J.T. Barer, 49%), anhydrous methanol (CH_3OH, Sigma-Aldrich, 99.99%), and chloroform ($CHCl_3$, Sigma-Aldrich, HPLC grade). Deionized (DI) water with a resistivity of 18.2 MΩ cm was used throughout. N-type (phosphorus doped, resistivity of 24−34 Ω cm) float-zone (FZ) Si(111) wafers with double sides polished were cut into 1.5 cm × 3.8 cm pieces for transmission mode infrared spectroscopy measurements.[13,14] The native oxide on the Si wafer was chemically cleaned with a 30 min exposure at 80 °C to a 1:3 solution of aqueous H_2O_2:18 M H_2SO_4. The wafer was then rinsed with DI water and dried under a steady stream of nitrogen. The Si(111) was H-terminated by a 30 s dip in aqueous 49% HF followed by a 2.5 min dip in aqueous 49% NH_4F, then carefully rinsed with DI water to remove any trace fluoride. This procedure produces a ⟨111⟩-oriented surface, atomically smooth for hundreds of nanometers.[15,16] These atomically flat surfaces were used as the starting substrate for functionalization using wet chemical methods. The wafers were immersed in anhydrous methanol (∼10 mL) in a closed glass vessel (V = 20 mL), backfilled with $N_2^{(g)}$, and refluxed at various temperatures (65−140 °C) for 12 h. At temperatures above reflux a pressure vessel was used. All experiments were performed in a $N_2^{(g)}$ purged glovebox.

Fourier Transform Infrared Spectroscopy (FT-IR). FT-IR experiments were performed in a $N_2^{(g)}$ purged glovebox on a Nicolet 6700 and obtained with a nominal 4 cm^{-1} resolution. Spectra were collected from 400 to 4000 cm^{-1} in transmission mode with an angle of incidence of 64° with respect to the silicon surface normal. A room-temperature pyroelectric detector (DTGS) was employed for data collection. In a typical experiment, 500 scans were taken and averaged over three loops.

Gas Chromatography Mass Spectrometry (GCMS). GCMS was performed on a Shimadzu QP2010-Plus gas chromatograph coupled with a mass spectrometer. The column of the GCMS is a Restek Rxi-5 ms column that consists of a stationary phase of 5% diphenyl/95% dimethyl polysiloxane. Samples were prepared by diluting a 0.10 mL aliquot of reacted methanol in 1.4 mL of HPLC grade chloroform. All analysis was run at 70 °C for 15 min retention in the chromatograph and then via mass spectrometry between 1 and 80 amu at a scan speed of 344.

Density Functional Theory (DFT) Calculations. All DFT calculations were performed using the generalized gradient approximation (GGA) as implemented in the Vienna ab initio simulation package (VASP).[17] The electron−ion interaction was described by the projector-augmented wave scheme,[18] where electronic wave functions were expanded into plane waves with kinetic energies up to 360 eV.[19] The surface was modeled by periodically repeated slabs, which consisted of 8 atomic layers of silicon with 3 × 3 surface periodicity in addition to adsorbed molecules and a vacuum region corresponding to 16 atomic layers. The seven uppermost silicon layers as well as the adsorbate degrees of freedom were allowed to relax until the atomic forces were below 10 meV/A. The Brillouin zone integration was performed using a 4 × 4 × 1 k-point mesh generated within the Monkhorst−Pack scheme. The PW91 functional was used to describe the electron exchange and correlation energy within the GGA.[20]

Vibrational eigenmodes and frequencies were calculated by the force-constant (FC) approach, diagonalizing the mass weighted second derivative matrix (Hessian) for the adsorbed species and the top Si layer. The restriction to the atoms of the top layer and the adsorbed species is legitimate because the eigenmodes localized at these atoms do not substantially overlap with the eigenmodes of the bulk material.

Kinetic barriers were calculated by the nudged elastic band (NEB) method, using a string of geometric configurations to describe the reaction pathway of the system. A spring interaction between every configuration ensured the continuity of the reaction pathway.

Kinetic Monte Carlo (kMC) Simulations. The present model uses the hexagonal geometry of the Si(111) surface lattice and assumes a perfect substrate without step edges. Periodic boundary conditions are implemented to account for the translational symmetry. The kMC algorithm takes into account adsorption and desorption processes, while diffusion is found to have no further impact due to the too high surface diffusion barrier. We are simulating adsorption and desorption events on the Si lattice. The probability p of each event depends on the state of its nearest neighbors. The probabilities for every event at each site during a cycle are

$$p^{\mathrm{desorp}}{}_{\mathrm{i}} = k^{\mathrm{desorp}}{}_{\mathrm{i}} \cdot dt \tag{1}$$

$$p^{\mathrm{adsorb}}{}_{\mathrm{i}} = k^{\mathrm{adsorb}}{}_{\mathrm{i}} \cdot dt \tag{2}$$

where $k^{\mathrm{desorp}}{}_{\mathrm{i}}$ and $k^{\mathrm{adsorb}}{}_{\mathrm{i}}$ are the rates of desorption and adsorption at each lattice site. These rates are recalculated at each cycle according to the state of lattice at the beginning of the cycle. Reaction rates k were calculated using DFT barrier values E (found in Table 1) in the transition state theory (TST) expression

$$k = (k_{\mathrm{B}}T/h) \cdot \mathrm{e}^{(-E/RT)} \tag{3}$$

Table 1. Calculated Energy Barriers for the Adsorption/Desorption Reaction of Methanol on the Si(111):H Surface as a Function of the Number of Methoxy Nearest Neighbors

number of methoxy nearest neighbors	barrier for adsorption/eV	barrier for desorption/eV
(0)	0.901	1.102
(1)	1.177	1.125
(2)	1.281	1.141
(3)	1.364	1.155
(4)	1.428	1.185
(5)	1.472	1.225
(6)	1.545	1.251

DOI: 10.1021/acs.jpcc.5b03816
J. Phys. Chem. C 2015, 119, 16947−16953

where k_B is the Boltzmann constant; T is the temperature; h is the Planck constant; and R is gas constant. This creates a dependency between events, and therefore we break the simulation into short cycles, such that in each cycle we have a very low density of events, guaranteeing that we do not have two adjutant events in one cycle. The number of events per cycle is

$$N_{events} = P_{events} N_{sites} \quad (4)$$

where P_{events} is the desired event density (typically 0.001) and N_{sites} is the number of sites in the simulated lattice. The simulated time duration of each cycle is

$$dt = N_{events}/(\Sigma k^{desorp}{}_i + \Sigma k^{adsorb}{}_i) \quad (5)$$

Equilibrium is reached when the number of adsorption and desorption events is the same or, in other words, when the density becomes constant apart from some random fluctuations.

RESULTS AND DISCUSSION

The adsorption study was performed by first determining the potential energy surface (PES) for single methoxy groups on the Si(111) surface. Apart from the fixed lateral position of the oxygen atom, the structural degrees of freedom of both the substrate and adsorbate were fully relaxed in these calculations.

Starting from the lowest energy adsorption configuration of a single methoxy unit on the Si(111):H surface unit cell, the methoxy coverage was systematically increased to nine methoxy units, corresponding to one monolayer. Here and in the following the notation Mn^l refers to structures with n methoxy units per unit cell and l describing the configuration of the methoxy−methoxy interaction (see Figure 1). The adsorption

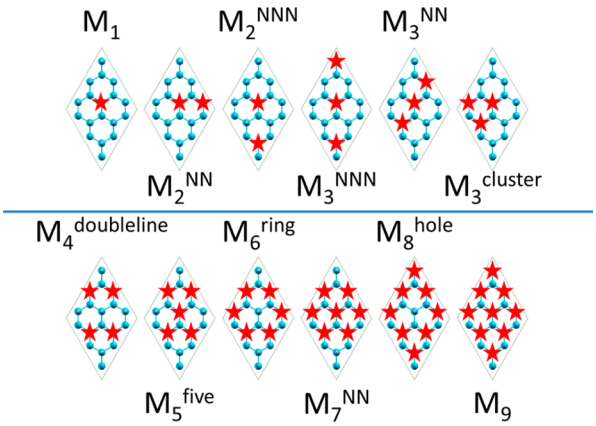

Figure 1. Most relevant configurations of the partial methoxy group (indicated by stars) Si(111):H surface considered here. In the notation Mn^l the number of methoxy groups is given by n, and l describes their configuration.

energy as a function of the number of methoxy units adsorbed on the Si(111):H surface following the chemical reaction

$$Si{-}H + nCH_3OH \leftrightarrows (Si{-}OCH_3)^l + nH_2 \quad (6)$$

has been calculated with respect to the methanol molecule in vacuum and the clean Si(111):H slab. However, the adsorption energy alone does not allow for a conclusion of the stability of a specific surface structure. The chemical potentials $\mu(A_i)$ of the surface constituents A_i must be taken into account to compare interfaces with different stoichiometries, i.e., a different number of molecules n_{A_i}, energetically. The ground state of the surface was determined by the minimum of the thermodynamic grand canonical potential

$$\Omega = F - \sum_i \mu(A_i) n_{A_i} \quad (7)$$

in dependence on the chemical potential μ of methanol and dihydrogen. Here F is the temperature-dependent surface free energy. When the number of adsorbed methoxy groups increases, their interaction becomes relevant and needs to be considered. In our unit cell, adsorbed methoxy groups can sit as nearest neighbor (NN) or next nearest neighbor (NNN). The most relevant configurations appearing in this study are shown in Figure 1.

Assuming a flat, i.e., stoichiometric, Si(111):H surface in the presence of methanol, the grand canonical potential depends on the chemical potentials of methanol and hydrogen. The calculated phase diagram for the thermodynamically stable methoxy-terminated Si(111) surface configurations that result from the reaction of methanol with the H-terminated Si(111) as a function of the methanol and hydrogen chemical potentials (see Figure 11 in ref 10) shows that the five-, the ring-, and the full methoxy-terminated phases of the Si(111) surface are thermodynamic favorable phases. The existence of a nanopattern containing precisely 1/3 methoxy and 2/3 H-termination with all methoxy groups as NNNs does not correspond to the thermodynamical ground state of the system, irrespective of the choice of the chemical potentials. The experimental findings reported in ref 5 thus cannot be explained by means of exclusively thermodynamic arguments. Therefore, kinetic effects and the influence of reaction barriers are investigated next.

Among the various conceivable reaction mechanisms for grafting of methanol on atomically smooth H-terminated Si(111), we have found the one illustrated in Figure 2 to be

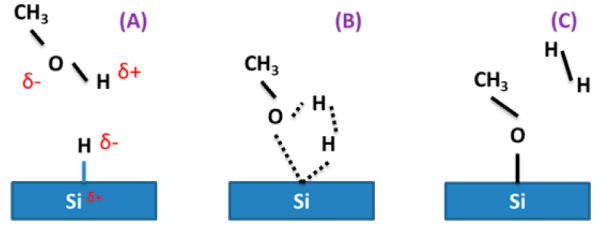

Figure 2. Suggested reaction mechanism for adsorption and desorption of methanol on Si(111):H.

the most favorable reaction pathway. As shown in Figure 2A, a methanol molecule approaches the H-terminated Si(111) before bond distortion occurs due to dipole−dipole interactions. Mutual attraction due to the Si−H and the −OH moieties' dipole moments increases the proximity of these terminal functional groups. Through a concerted reaction step near the transition state the new Si−O and H−H bonds become stronger (see Figure 2B), while existing bonding becomes weaker. In the final electron transfer, the alkoxide is covalently grafted to the silicon surface, and dihydrogen is released (see Figure 2C).

This reaction pathway profits from the flexibility of the silicon atoms in the top of the lattice, thus reducing the kinetic barriers due to the concerted nature of the reaction mechanism by ∼1 eV. These processes have been well documented in the

DOI: 10.1021/acs.jpcc.5b03816
J. Phys. Chem. C 2015, 119, 16947−16953

literature as lattice-assisted transitions and may be enhanced if temperature is increased, thus promoting silicon phonon modes.[21] These effects are a consequence of the localized nature of the covalent bonds of silicon. As shown in Table 1, the resulting energy barriers of the aforementioned reaction pathway are dependent on the number of next neighbors methoxy groups on the surface. The adsorption process becomes more likely when the number of methoxy groups in nearest neighbor configurations is low. The main reason for the increase of the energy barrier with increasing number of nearest neighbor methoxy groups is an attraction of methanol with a higher number of methoxy nearest neighbors. This effect is not found for the back reaction. Second, with an increasing coverage of methoxy groups the relaxation of the transition state is sterically hindered.

The DFT generated information regarding the reaction mechanism has been implemented in a kMC algorithm. Representative kMC images of the reaction process of methanol with H-terminated Si(111) at 65 °C are shown in Figure 3. The time is evolving from A to L. The methoxy groups initially adsorb randomly, and a further ordering process is excluded due to the too high surface diffusion barrier. When the coverage of ∼0.3 ML is reached, the surface starts to self-order during the dynamically performed adsorption and desorption processes. At 65 °C the surface ends up with a coverage ∼0.3 ML methoxy groups and a total number of nearest neighbors close to 0. This corresponds obviously to the nanopattern detected experimentally in ref 5 after the system has reached equilibrium. We mention that evidence for the suggested reaction mechanism is provided by the experiment being performed with deuterated methanol. It shows that the Si−H stretch vibration is replaced by a Si−D stretch.[5]

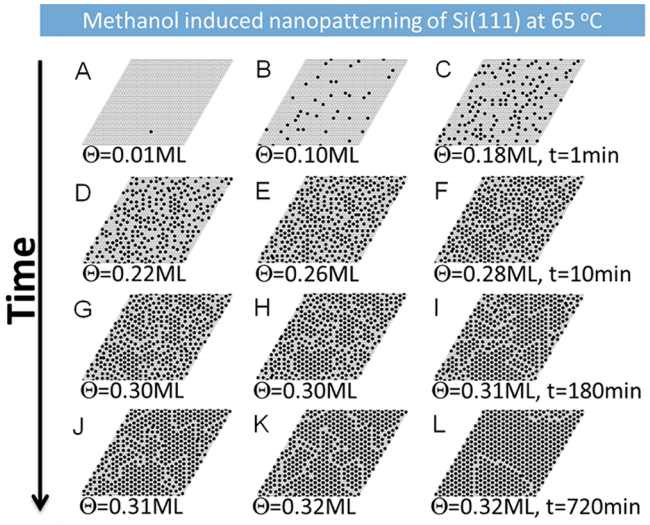

Figure 3. Representative kMC images of the reaction process of methanol with H-terminated Si(111) at 65 °C. Time evolves from A to L. First, the methoxy groups adsorb randomly, and a further ordering process is excluded due to the too high surface diffusion barrier. When the coverage of ∼0.3 ML is reached, the surface starts to self-order as a result of the dynamically performed adsorption and desorption processes.

The next questions to be addressed are (i) does the nanopattern depend on temperature and (ii) what are the implications of a temperature-dependent surface modification on the experimental signature?

Variable-temperature surface methoxylation reactions were performed to assess the temperature dependence of the nanopatterning. After each reaction the surface was analyzed with FT-IR spectroscopy (see Figure 4). Michalak et al. have shown that methanol reacting with Si(111):H under refluxing conditions for 12 h yields 30% of a monolayer with six covalently bound hydrogen atoms as nearest neighbors. Atomically smooth Si(111):H was reacted with methanol at different variable temperatures for a fixed period of time in a $N_2^{(g)}$-purged glovebox. Figure 4 depicts the temperature-dependent spectra where all the vibrational modes ascribable to Si−OCH_3 species are present. These are the Si−O stretching mode at 734 cm^{-1}, the Si−O−C stretching mode at 1080 cm^{-1}, the CH_3 umbrella mode at 1180 cm^{-1}, the symmetric CH_3 stretching mode at 2832 cm^{-1}, and the two nondegenerate asymmetric CH_3 stretching modes at 2975 and 2942 cm^{-1}.

Figure 4 (rhs) shows the influence of the temperature on the Si−H stretch mode around ∼2080 cm^{-1}. As we will show below, the peak modification of the Si−H stretch peak with temperature indicates that the influence of the reaction barriers weakens, and the nanopatterned surface gets increasingly disordered.

The emergence of new peaks at 140 °C detected here provides strong evidence for the decomposition of methanol and the formation and adsorption of new chemical moieties on the surface. Experimental evidence yields a change of methoxy group coverage as a function of temperature, while the composition of methanol was shown to be temperature dependent. The formation of new chemical moieties as shown by FT-IR spectroscopy leads us to believe that the decomposition of methanol is an important factor which has to

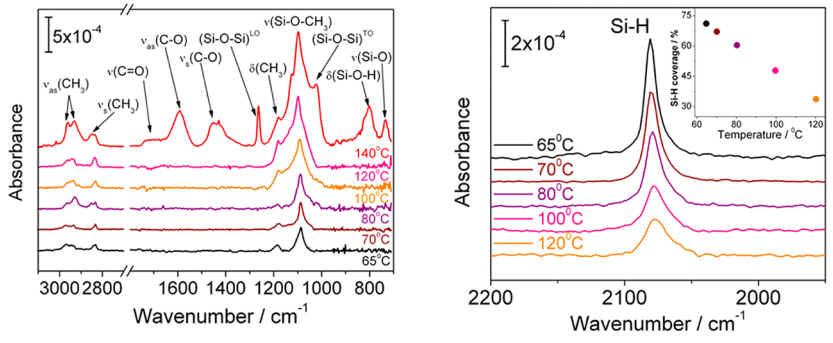

Figure 4. Representative FT-IR spectra after immersion of atomically smooth H-terminated Si(111) surfaces in neat anhydrous CH_3OH for 12 h at different temperatures.

DOI: 10.1021/acs.jpcc.5b03816
J. Phys. Chem. C 2015, 119, 16947−16953

be taken into account. The composition of methanol as a function of temperature was investigated using a microkinetic model as shown in Figure 5. We have investigated the chemical

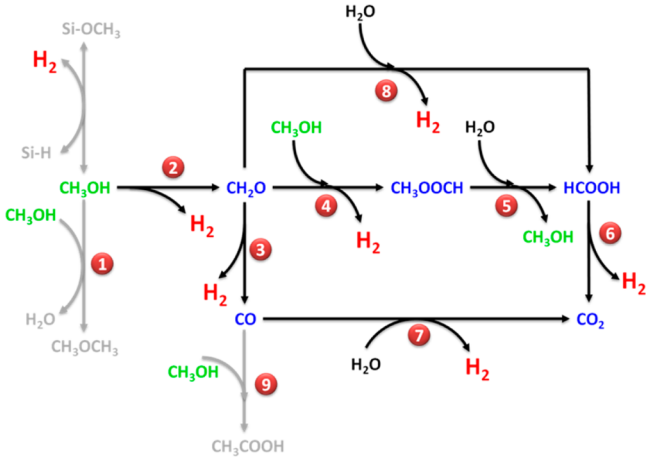

Figure 5. Scheme of the most relevant reactions that methanol can undergo in a closed system. Reactions 1 to 9 represent steps of decomposition.

composition of methanol as a function of temperature based on the nine chemical reactions, namely

$$2CH_3OH \leftrightarrows H_2O + CH_3OCH_3 \quad (1)$$

$$CH_3OH \leftrightarrows CH_2O + H_2 \quad (2)$$

$$CH_2O \leftrightarrows CO + H_2 \quad (3)$$

$$CH_2O + CH_3OH \leftrightarrows H_2 + CH_3OOCH \quad (4)$$

$$CH_3OOCH + H_2O \leftrightarrows CH_3OH + CHOOH \quad (5)$$

$$CHOOH \leftrightarrows CO_2 + H_2 \quad (6)$$

$$CO_2 + H_2 \leftrightarrows CO + H_2O \quad (7)$$

$$CH_2O + H_2O \leftrightarrows H_2 + CHOOH \quad (8)$$

$$CO + CH_3OH \leftrightarrows CH_3COOH \quad (9)$$

Kinetic barriers were calculated for each reaction using the nudged elastic band (NEB) method. The values are given in Table 2. Reaction rate constants for reactions were calculated using DFT barrier values in the transition state theory (TST) expression. The chemical composition of the methanol is calculated then in steady-state approximation and shown in Figure 6 (lhs). It can be seen that at temperatures higher than 100 °C the products of the chemical decomposition of methanol start to initiate oxidation of the silicon wafer, in agreement with the experimental FT-IR findings.

Table 2. Calculated Energy Barriers of the Chemical Decomposition of Gas-Phase Methanol[a]

number of reaction	barrier for reaction/eV	barrier for back-reaction/eV
(1)	3.293	3.492
(2)	4.227	2.892
(3)	3.903	3.653
(4)	2.585	3.005
(5)	3.137	2.756
(6)	3.126	3.167
(7)	5.311	4.982
(8)	2.943	2.981
(9)	2.187	2.610

[a]The notation of the reactions refers to Figure 5.

We also performed chromatography mass spectrometry (GCMS). The GCMS spectra shown in Figure 6 (rhs) contrast two samples of methanol: a nonpreheated vs a preheated sample. The peak intensities of the chromatography allow us to conclude on the concentration of the sample, while the width of the peaks gives information on the alteration of the chemical compositions and their extended interactions with the stationary phase of the column. If there is any change in the chemical composition of the methanol, the retention time will be modified. As one can see in the case of the nonpreheated methanol sample, the retention time (width of the peak) is small, while for the preheated sample, the retention time is much longer (width of the peak is wider). This gives evidence of a change in the chemical composition of the methanol during the heating.

For the chemical reaction of methanol with the H-terminated Si(111) we find the temperature and its effect on the hydrogen chemical potential to affect most strongly the kinetics of the system. This leads us automatically to the discussion of the limits of the equilibrium exchange reaction model. The reaction does not take place for temperatures close to room temperature. At 65 °C the chemical potential of hydrogen is sufficiently high for the system to reach the dynamic equilibrium of the exchange reaction. At temperatures above 100 °C, the products of the chemical decomposition (namely, water, formaldehyde, methylformate, and formic acid) of methanol start to initiate oxidation of the silicon wafer; further studies are necessary here.

Finally, we want to prove that the combination of theoretical and experimental tools chosen here is in fact adequate to resolve such a complex adsorbate system and may be used to uncover lateral resolution and spatial ordering of the molecules. Therefore, we studied a test system where the methoxy groups are replaced by fluorine groups. This reduces the number of degrees of freedom of the structures that need to be considered in the calculation. Because of the periodic boundary conditions, it is necessary to use a large unit cell. Figure 7 depicts three structures, the fully H-terminated Si(111) surface (lhs), the Si(111) surface with an ordered, periodic arrangement of 1/3 ML fluorine- and 2/3 ML H-termination (middle), and the Si(111) surface with a disordered coverage of 1/3 ML fluorine- and 2/3 ML H-termination (rhs). In the ordered structure in the middle every fluorine group is surrounded by six Si−H groups standing as nearest neighbors (NNs) and six fluorine groups standing as next nearest neighbors (NNNs), resembling the nanopatterned surface discussed above. Can the periodic and the disordered structure (same coverage) be distinguished by means of FT-IR? In Figure 8 (top) the calculated infrared spectra for the Si−H stretch vibration of the three surface structures depicted in Figure 7 are shown. In the case of the Si(111) surface with a periodic coverage of 1/3 ML fluorine- and 2/3 ML H-termination, the calculated Si−H stretch mode is shifted to higher wavenumbers, and the intensity is reduced (∼1/3 reduced). Interestingly, in the case of the Si(111) surface with a disordered coverage of 1/3 ML fluorine- and 2/3 ML H-termination, the peak becomes broader and shows an asymmetric distortion toward lower wavenumbers. This observation is helpful for the interpretation of the experimental

DOI: 10.1021/acs.jpcc.5b03816
J. Phys. Chem. C 2015, 119, 16947−16953

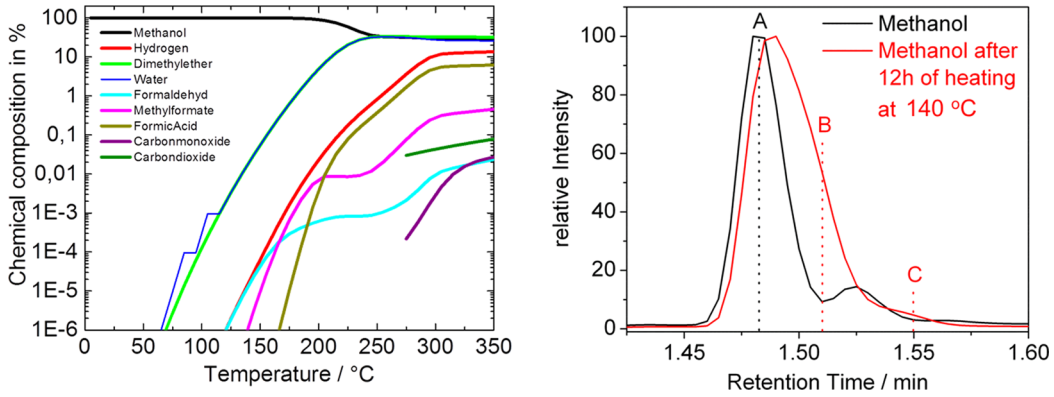

Figure 6. (lhs) Chemical composition of gas-phase methanol as a function of temperature, calculated in steady-state approximation. (rhs) GCMS shown for preheated and nonpreheated methanol, respectively. For the nonpreheated methanol sample (black line), the retention time (width of the peak) is small, while for the preheated sample (red line), the retention time is much longer (width of the peak is wider).

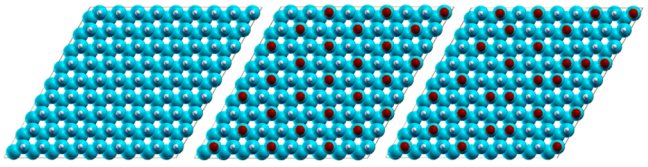

Figure 7. Top view of clean Si(111):H surface (lhs) and Si(111) surface with an ordered (middle) and random (rhs) arrangement of 1/3 ML fluorine- and 2/3 ML H-termination. In the arrangement, i.e., the nanopatterned surface, every fluorine group is surrounded by six Si−H groups standing as nearest neighbors (NNs) and six fluorine groups standing as next nearest neighbors (NNNs).

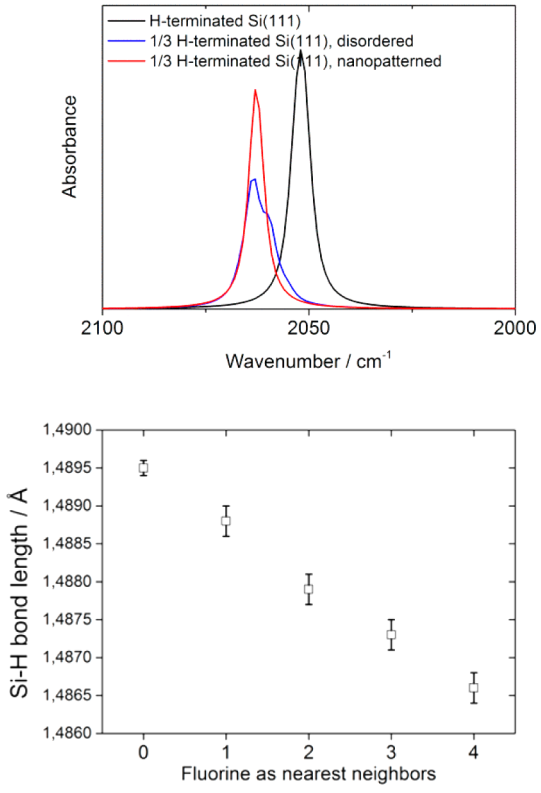

Figure 8. (top) Calculated infrared spectra of the Si−H stretch vibration of the Si(111):H surface (black) and the Si(111) surface with an ordered (red) and random (blue) arrangement of 1/3 ML fluorine- and 2/3 ML H-termination. (bottom) Si-H bond length as a function of the numbers of fluorine nearest neighbors.

FT-IR data in Figure 4. Here with a rising temperature the peak becomes asymmetric into the direction of low wavenumbers. This corroborates our theoretical conclusion above that at low temperature the access to the thermodynamic ground state is kinetically hindered. With rising temperature, however, the influence of the reaction barriers weakens, and the nanopatterned surface gets increasingly disordered. The consideration of the fluorine group covered model systems thus provides additional evidence for our hypothesis that the nanopatterned OCH_3-terminated Si(111) surface corresponds to kinetically restricted surface structure rather than the thermodynamic ground state.

CONCLUSIONS

In this manuscript we have reinvestigated the formation of a nanopattern during the surface reaction of methanol with H-terminated Si(111). Methanol reacts with H-terminated Si(111) under the release of hydrogen. The activation barrier is moderate and depends on the number of methoxy group neighbors.

The existence of a nanopattern consisting precisely of 1/3 methoxy and 2/3 H-termination with all methoxy groups as next nearest neighbors cannot be explained using thermodynamics exclusively. At 65 °C the system is not yet at thermodynamic equilibrium; i.e., the temperature is not sufficiently high to overcome local kinetic barriers and reach the most stable state.

Therefore, the possibility of desorption in the nanopattern mechanism and thus establishing a dynamic equilibrium was considered. Our experimental results (FT-IR and GCMS) give evidence for a change in methoxy group coverage as a function of temperature between 65 and 140 °C. In temperature regimes around room temperature, the reaction does not take place. At 65 °C the chemical potential of hydrogen is high enough and the system reaches the dynamic equilibrium of the exchange reaction. At temperatures above 100 °C, the products of the chemical decomposition (namely, water, formaldehyde, methylformate, and formic acid) of methanol start to initiate oxidation of the silicon wafer.

The nanopattern formation is successfully modeled with kMC simulations with input parameters taken from DFT total-energy calculations. The simulations explain the nanopattern as resulting from an ordering process accompanying the adsorption and desorption reactions due to the dependence

DOI: 10.1021/acs.jpcc.5b03816
J. Phys. Chem. C 2015, 119, 16947−16953

of the adsorption/desorption barriers on the occupation of the neighboring bonding sites on the Si surface.

AUTHOR INFORMATION

Corresponding Author

*E-mail: peter.thissen@kit.edu.

Notes

The authors declare no competing financial interest.

ACKNOWLEDGMENTS

PT and WGS thank the DFG for financial support. The authors acknowledge the Texas Advanced Computing Center (TACC) for computational resources.

REFERENCES

(1) Aswal, D. K.; Lenfant, S.; Guerin, D.; Yakhmi, J. V.; Vuillaume, D. Self-Assembled Monolayers on Silicon for Molecular Electronics. *Anal. Chim. Acta* **2006**, *568*, 84−108.

(2) Buriak, J. M. Organometallic Chemistry on Silicon and Germanium Surfaces. *Chem. Rev.* **2002**, *102*, 1271−1308.

(3) Love, J. C.; Estroff, L. A.; Kriebel, J. K.; Nuzzo, R. G.; Whitesides, G. M. Self-Assembled Monolayers of Thiolates on Metals as a Form of Nanotechnology. *Chem. Rev.* **2005**, *105*, 1103−1169.

(4) Lenz, T.; Schmaltz, T.; Novak, M.; Halik, M. Self-Assembled Monolayer Exchange Reactions as a Tool for Channel Interface Engineering in Low-Voltage Organic Thin-Film Transistors. *Langmuir* **2012**, *28*, 13900−13904.

(5) Michalak, D. J.; Amy, S. R.; Aureau, D.; Dai, M.; Esteve, A.; Chabal, Y. J. Nanopatterning Si(111) Surfaces as a Selective Surface-Chemistry Route. *Nat. Mater.* **2010**, *9*, 266−271.

(6) Michalak, D. J.; Amy, S. R.; Esteve, A.; Chabal, Y. J. Investigation of the Chemical Purity of Silicon Surfaces Reacted with Liquid Methanol. *J. Phys. Chem. C* **2008**, *112*, 11907−11919.

(7) Michalak, D. J.; Rivillon, S.; Chabal, Y. J.; Esteve, A.; Lewis, N. S. Infrared Spectroscopic Investigation of the Reaction of Hydrogen-Terminated, (111)-Oriented, Silicon Surfaces with Liquid Methanol. *J. Phys. Chem. B* **2006**, *110*, 20426−20434.

(8) Longo, R. C.; Cho, K.; Schmidt, W. G.; Chabal, Y. J.; Thissen, P. Monolayer Doping via Phosphonic Acid Grafting on Silicon: Microscopic Insight from Infrared Spectroscopy and Density Functional Theory Calculations. *Adv. Funct. Mater.* **2013**, *23*, 3471−3477.

(9) Thissen, P.; Peixoto, T.; Longo, R. C.; Peng, W.; Schmidt, W. G.; Cho, K.; Chabal, Y. J. Activation of Surface Hydroxyl Groups by Modification of H-Terminated Si(111) Surfaces. *J. Am. Chem. Soc.* **2012**, *134*, 8869−8874.

(10) Thissen, P.; Seitz, O.; Chabal, Y. J. Wet Chemical Surface Functionalization of Oxide-Free Silicon. *Prog. Surf. Sci.* **2012**, *87*, 272−290.

(11) Thissen, P.; Vega, A.; Peixoto, T.; Chabal, Y. J. Controlled, Low-Coverage Metal Oxide Activation of Silicon for Organic Functionalization: Unraveling the Phosphonate Bond. *Langmuir* **2012**, *28*, 17494−17505.

(12) Solares, S. D.; Michalak, D. J.; Goddard, W. A.; Lewis, N. S. Theoretical Investigation of the Structure and Coverage of the Si(111)-OCH_3 Surface. *J. Phys. Chem. B* **2006**, *110*, 8171−8175.

(13) Stefanov, B. B.; Gurevich, A. B.; Weldon, M. K.; Raghavachari, K.; Chabal, Y. J. Silicon Epoxide: Unexpected Intermediate During Silicon Oxide Formation. *Phys. Rev. Lett.* **1998**, *81*, 3908−3911.

(14) Weldon, M. K.; Stefanov, B. B.; Raghavachari, K.; Chabal, Y. J. Initial H_2O-Induced Oxidation of Si(100). *Phys. Rev. Lett.* **1997**, *79*, 2851.

(15) Dumas, P.; Chabal, Y. J. Electron-Energy-Loss Characterization of the H-Terminated Si(111) and Si(100) Surfaces Obtained by Etching in NH_4F. *Chem. Phys. Lett.* **1991**, *181*, 537−543.

(16) Higashi, G. S.; Chabal, Y. J.; Trucks, G. W.; Raghavachari, K. Ideal Hydrogen Termination of the Si (111) Surface. *Appl. Phys. Lett.* **1990**, *56*, 656−658.

(17) Kresse, G.; Furthmuller, J. Efficient Iterative Schemes for Ab Initio Total-Energy Calculations Using a Plane-Wave Basis Set. *Phys. Rev. B* **1996**, *54*, 11169−11186.

(18) Kresse, G.; Joubert, D. From Ultrasoft Pseudopotentials to the Projector Augmented-Wave Method. *Phys. Rev. B* **1999**, *59*, 1758−1775.

(19) Kresse, G.; Furthmuller, J. Efficiency of Ab-Initio Total Energy Calculations for Metals and Semiconductors Using a Plane-Wave Basis Set. *Comput. Mater. Sci.* **1996**, *6*, 15−50.

(20) Perdew, J. P.; Chevary, J. A.; Vosko, S. H.; Jackson, K. A.; Pederson, M. R.; Singh, D. J.; Fiolhais, C. Atoms, Molecules, Solids, and Surfaces - Applications of the Generalized Gradient Approximation for Exchange and Correlation. *Phys. Rev. B* **1992**, *46*, 6671−6687.

(21) Xia, J. B.; Gan, Z. Z., Han, R. Q.; Qin, G. G.; Yang, G. Z.; Zheng, H. Z.; Zhong, Z. T.; B. F. Zhu *Lattice Dynamics and Semiconductor Physics: Festschrift for Professor Kun Huang*; World Scientific Publishing Co. Pte. Ltd.: New Jersey, 1990; p 500.

DOI: 10.1021/acs.jpcc.5b03816
J. Phys. Chem. C 2015, 119, 16947−16953